The Journal of Nutrition 154 (2024) 1175–1188

American Society for Nutrition
Excellence in Nutrition Research and Practice

JN THE JOURNAL OF NUTRITION

journal homepage: https://jn.nutrition.org/

Nutrient Physiology, Metabolism, and Nutrient-Nutrient Interactions

In-Ovo Glutamine Administration Enhances Intestinal Development and Functions in Broiler Chickens: Insights from Enteroid Models

Liang-en Yu [1], Peter Mann [1], Lydia Schlitzkus [2], Federico Ghiselli [3], Mia Sanders [1], Abdallah Hadimundeen [1], Yihang Li [1,2,*]

[1] *Department of Animal and Food Sciences, University of Delaware, Newark, DE, United States;* [2] *Department of Biological Sciences, University of Delaware, Newark, DE, United States;* [3] *Department of Veterinary Medical Sciences, University of Bologna, Bologna, Italy*

A B S T R A C T

Background: Early life events play significant roles in tissue development and animal health in their later life. Early nutrition, through in-ovo delivery, has shown beneficial effects on improving intestinal health in broiler chickens. However, the underlying mechanism is not fully investigated. A recently developed enteroid culture technique allows investigations on intestinal epithelial functions that are close to physiologic conditions.

Objectives: In this study, we evaluated the short- and long-term effects of in-ovo administration of glutamine (Gln) on intestinal epithelial development and functions by using intestinal enteroid culture and tissue electrophysiologic analysis.

Methods: A hundred eggs of commercial Cobb500 broilers were in-ovo injected with 0.2 mL of either phosphate-buffered saline (PBS) or 3% Gln at embryonic day 18 (E18). Chicks were killed on the day of hatch, and at 3- and 14-d posthatch. Enteroids were generated from the small intestine. After 4 d of culture, enteroids were harvested for 5-ethynyl-2′-deoxyuridine proliferation, fluorescein isothiocyanate-4 kDa dextran permeability, and glucose absorption assays. At day 3 (d3) and day 14 (d14), intestinal barrier and nutrient transport functions were measured by the Ussing chamber. The gene expression of epithelial cell markers, nutrient transporters, and tight-junction proteins were analyzed in both intestinal tissues and enteroids.

Results: In comparison with the PBS control group, in-ovo Gln increased intestinal villus morphology, epithelial cell proliferation, and differentiation, and altered epithelial cell population toward increased number of enteroendocrine and goblet cells while decreasing Paneth cells. Enteroids gene expression of nutrient transporters (B0AT1, SGLT1, and EAAT3), tight junction (ZO2), glucose absorption, and barrier functions were enhanced on the day of hatch. Long-term increases of intestinal di-peptide and alanine transport were observed at day 14 posthatch.

Conclusions: Together our results suggested that the in-ovo injection of Gln stimulated intestinal epithelium proliferation and programmed the epithelial cell differentiation toward absorptive cells.

Keywords: broilers, enteroids, glutamine, gut health, intestinal barrier, intestinal nutrient transporter, in-ovo injection

Introduction

Early life nutrition during the peri-hatching period plays significant roles in intestinal development in modern broiler chickens. The embryonic development period is responsible for >30% of the whole lifespan of commercial broiler chickens [1]. During the last 3 d prehatch and first 3 d posthatch, the weight of the intestine increased 3.5-fold [2,3]. Unlike mammals that receive nutrients via the placenta, the nutrient supply for a chicken embryo could be limited by the size of the egg, which is the sole source supporting organ development. Therefore, early

Abbreviations: 2-NBDG, 2-(N-(7-Nitrobenz-2-oxa-1,3-diazol-4-yl)Amino)-2-Deoxyglucose; ATB0, amino acid transporter B^0; B0AT, B0 amino acid transporter; BW, body weight; ChgA, chromogranin A; DAPI, 4′,6-diamidino-2-phenylindole; Dll, delta-like canonical Notch ligand; EAAT, excitatory amino acid transporter; EdU, 5-ethynyl-2′-deoxyuridine; EEC, enteroendocrine cell; FD4, fluorescein isothiocyanate-4 kDa dextran; FOM, floating organoid medium; Gln, glutamine; GLUT2, glucose transporter 2; Hes1, hes family bHLH transcription factor 1; IESC, intestinal epithelial stem cells; Isc, short-circuit current; Lgr5, leucine-rich repeat containing G protein-coupled receptor 5; LN_2, liquid nitrogen; LYZ, lysozyme; Muc2, mucin 2; OCLN, occludin; OCT, optimal cutting temperature compound; Olfm4, olfactomedin 4; PAS, periodic acid-Schiff; PBS, phosphate-buffered saline; PCNA, proliferating cell nuclear antigen; PepT1, peptide transporter 1; PFA, paraformaldehyde; RPL1, ribosomal protein lateral stalk subunit P1; RPL4, ribosomal protein L4; SGLT1, sodium-glucose linked transporter; TBP, TATA-box binding protein; TER, transepithelial resistance; Thr, threonine; ZO, zonula occludens.

* Corresponding author. *E-mail address:* liyh@udel.edu (Y. Li).

https://doi.org/10.1016/j.tjnut.2024.02.007
Received 17 October 2023; Received in revised form 1 February 2024; Accepted 7 February 2024; Available online 13 February 2024

nutrition programming has been suggested as a strategy to improve intestinal development [4]. In-ovo administration of carbohydrates or amino acids has shown beneficial effects on intestinal development in poultry, including improved jejunum morphology in pigeons and broilers [5–7], as well as increased intestinal weight and digestive enzymes in geese [8], chickens [9], and ducks [10]. However, less is known regarding how the in-ovo nutrition influences intestinal epithelial functions, such as nutrient transport, barrier, and enteroendocrine.

Optimal intestinal functions rely on the maturation of epithelial cell populations, such as enterocytes, goblet cells, Paneth cells, enteroendocrine cells (EECs), and the activity of their progenitor cells and epithelial stem cells (IESC) [11,12]. Intestinal epithelial cell-specific gene markers, such as delta-like canonical Notch ligand 1 (Dll1) (secretory progenitor cells), hes family bHLH transcription factor 1 (Hes1) (absorptive progenitor cells), mucin 2 (Muc2) (goblet cells), chromogranin A (ChgA) (EECs), lysozyme (LYZ) (Paneth cells), olfactomedin 4 (Olfm4), and leucine-rich repeat containing G protein-coupled receptor 5 (Lgr5) (IESC) have been widely used to estimate epithelial turnover and maturation directions [13–15]. However, the evaluation of these cell functions in avian species, especially during the peri-hatch period, has been understudied because of the lack of appropriate cell models. A recently developed enteroid model, derived from the chicken embryonic small intestine, has shown promising properties representing intestinal cell populations [16]. These 3D apical-out enteroids recapitulate the structure of the intestinal epithelium and allow convenient analysis of the intestinal barrier and nutrient transport functions.

Glutamine (Gln) serves as one of the major fuels for the intestinal epithelium and regulates epithelial cell proliferation, barrier function, apoptosis, and inflammation [17]. In-ovo Gln administration stimulated intestinal cell proliferation and differentiation in chickens [18]. However, how early life Gln impacts immediate gut function at hatch and at later posthatch life has not been fully evaluated.

In this study, we conducted in-ovo Gln injection to E18 broiler chicken embryos and monitored intestinal epithelial cell population changes by cell-specific marker gene expression and immunofluorescent staining. We further evaluated intestinal functions on the day of hatch by using apical-out enteroid analysis and evaluated later posthatch intestinal functions by using Ussing chamber electrophysiologic analysis. Our data indicated that the early life Gln in-ovo nutrition accelerated the development and maturation of the intestinal epithelium in both the short- and long-term posthatch.

Methods

Animal procedure and in-ovo Gln administration

All animal care procedures were approved by the University of Delaware Institutional Animal Care and Use Committee. A total of 100 Cobb 500 fertile eggs were obtained from the same laying flock in a local hatchery to minimize maternal variations. The eggs were incubated at 37.5°C and 60% humidity for 21 d. On embryonic day 18 (E18), the eggs were randomly assigned into 2 groups of in-ovo injections: phosphate-buffered saline (PBS) control and Gln supplementation. Starting from E18, the shift of yolk nutrient absorption pathway (from yolk sac membrane to the yolk stalk) allows specific delivery of exogenous nutrients directly into gut lumen of the middle intestine [19]. Therefore, the in-ovo Gln injection site was targeted on the yolk sac in this study. Before injection, the eggshell was sterilized with 70% ethanol. One dose of 200 μL sterile PBS (1X) or Gln (200-mM, G3126, Sigma) was gently injected into the yolk via a 23-G 1.5-inch needle. The injection hole was subsequently sealed with glue. Eggs were further incubated till day E21. Immediately after hatch, the chicks were transferred to environmentally controlled isolators. Birds were fed with a commercial broiler starter diet and were raised following industrial standards (24 h light) till 14 d of age. Individual body weight (BW) and group feed intake were recorded at d3, d7, and d14 of age.

Sample collection

On the day of hatch, in addition to d3 andd14 posthatch, birds were killed by decapitation or cervical dislocation. The entire intestine from duodenum to cloaca was collected and linearized by removing the mesentery. The total length of the intestine was measured. The distal ileum was fixed in 4% paraformaldehyde (PFA) for later histology and immunohistochemistry staining. The proximal ileum was snap frozen in liquid nitrogen (LN_2) for later gene expression analysis. On the day of hatch, the middle ileum from 3 embryos was harvested and pooled together for the isolation of villus units and enteroids development. At d3 and d14 posthatch, the middle ileum was harvested for Ussing chamber analysis.

Histology analysis

PFA-fixed-ileum tissues were washed 3 times by PBS, and then dehydrated overnight in 30% sucrose. After dehydration, the tissues were embedded in optimal cutting temperature compound and cryosectioned into 10 μm-thick sections mounted on slides. The slides were stained with hematoxylin and eosin. Tissue histologic images were obtained under a bright field microscope. The villus height, crypt depth, and crypt fission were measured via ImageJ software (NIH). The identifications of crypt fission and villus–crypt measurements were based on previous research [20,21]. The crypt fission rate was calculated by counting the number of bifid crypts and dividing by the total number of crypts, which was expressed as a percentage of bifid crypts.

Alcian-Blue staining

Fixed-ileum tissue slides were stained with a commercial Alcian-Blue periodic acid-Schiff (PAS) Stain Kit (ab245876, Abcam). Images were obtained under a bright field microscope and villus height, crypt depth, and positive-stained cells numbers were measured via ImageJ software (NIH,). The goblet cell number was normalized to the total length of a villus–crypt axis.

Immunofluorescence staining

Tissue slides were washed with PBS and permeabilized via 0.1% Triton-X (T8787, Sigma). After blocking with 0.5% bovine serum albumin, the tissue slides were incubated with anti-LYZ (PA5-16668, Invitrogen) or anti-ChgA (MA513096, Invitrogen) primary antibodies. Followed by washing off primary antibodies, the slides were incubated with secondary anti-rabbit IgG antibody (G21234, Invitrogen) or anti-mouse IgG antibody (A32723, Invitrogen) respectively. 4′,6-diamidino-2-phenylindole (DAPI)

(P36931, Invitrogen) was used to label the nuclei of cells. Images were obtained under a fluorescent microscope. The number of positively stained (LYZ for Paneth cell, ChgA for EEC) cells was counted by ImageJ software (NIH). The region-specific LYZ and ChgA positive cell numbers were normalized on the basis of crypt depth, upper and lower half of the villus height, and the total length of the villus–crypt axis.

Intestinal villus units isolation and apical-out enteroid culture

The intestinal villus unit isolation procedure was modified from previous research [16,22]. Briefly, the chick embryos were killed via decapitation on embryonic day 21. The middle ileum segments (3–4 cm length) were collected and washed with ice-cold Dulbecco's phosphate buffered saline (DPBS, 21-031-CV, CORNING). The ileum segments were minced into 0.5-cm pieces and digested in Dulbecco's Modified Eagle Medium (DMEM/F12, 12634010, Gibco) with 0.2 mg/mL collagenase (C9891, Sigma) and 6-μM Y27632 (1254, TOCRIS) at 37°C for 30 min. The villus units were released after vigorous shaking. The desired size of villus units (40–100 μm) was collected and uniformed through cell strainers. A portion of isolated villus units were immediately cultured in the floating organoid medium (FOM), which contained 10-mM HEPES (15630106, Gibco), 2-mM L-glutamine (G-3126, Sigma), 50 U/mL P/S (15140122, Gibco), and 2% B27 (12587010, Gibco) in DMEM/F12 media. Other villus units were cryopreserved in a freezing media consisting of 10% Dimethyl sulfoxide (DMSO, D2650, Sigma) and 90% FOM and stored in LN_2 for later use.

The enteroid culture procedure was conducted according to previous publications with modifications [16,22]. Briefly, sphere-shape enteroids were formed after 24-h culture of the isolated villus units in the FOM media. To avoid contamination of adherent cells, after 48-h in culture, the floating enteroids were collected, and centrifuged at 300 × *g* for 5 min at 4°C. Enteroid pellets were resuspended in FOM and cultured in standard cell culture-treated plates at a density of 800 enteroids per mL. Half of the media was replaced in each well every 2 d. After 4 d of culture, the enteroids were harvested for further analysis. The individual chicken embryo was used as an experimental unit. A total of 6–12 replicates were included.

qRT-PCR analysis

The mRNA expression levels of DII1, Hes1, proliferating cell nuclear antigen (PCNA), ChgA, MUC2, LYZ, Lgr5, Olfm4, zonula occludens (ZO2), occludin (OCLN), TJP1, sodium-glucose linked transporter (SGLT1), glucose transporter 2 (GLUT2), excitatory amino acid transporter (EAAT3), B0 amino acid transporter 1 (B0AT1), TATA-box binding protein (TBP), ribosomal protein lateral stalk subunit P1 (RPL1), and ribosomal protein L4 (RPL4) were determined by qRT-PCR. The detailed primer information is shown in Table 1. The total RNA of frozen ileum samples was isolated by Trizol reagent (T9424, Sigma), according to the manufacturer's instructions. After isolation, total RNA concentration was measured through nanodrop (13400525, Thermo Fisher Scientific). The cDNA was synthesized by a commercial kit (K1672, Thermo Fisher Scientific). qRT-PCR was performed in a QuantStudio 3 Real-Time PCR Detection System (Applied Biosystems) with 2× SYBR qPCR Mix (A25742, Applied Biosystems). The comparative Ct method ($2^{-\Delta\Delta CT}$ method) was used to quantify gene expression with the genes TBP, RPL1, and RPL4 served as internal controls [23].

Enteroids EdU proliferation analysis

The proliferation of enteroids was measured via a commercial 5-ethynyl-2′-deoxyuridine (EdU) HTS kit (BCK-HTS488-2, base click). Briefly, the EdU molecule was incubated with enteroids for 2 h at 37°C with 5% CO_2. The enteroids were washed and fixed with 4% PFA, followed by 0.1% Triton-X permeabilization. The EdU was labeled via kit reagents. Cell nuclei were stained with DAPI (10236276001, Sigma). The fluorescent intensity of EdU and DAPI were quantified under Excitation/Emission wavelengths 496/516 nm and 340/488 nm, respectively. The proliferation was indicated as the ratio of EdU to DAPI intensity.

Enteroid fluorescein isothiocyanate-4 kDa dextran (FD4) permeability analysis

FD4 (46944, Sigma) was used for FD4 permeability assay as described previously [22]. Briefly, enteroids were treated with 2 mg/mL FD4 at 37°C for 2 h. After treatment, the residual FD4 in the medium was removed via ice-cold PBS wash, followed by 300 × *g* centrifugation at 4°C for 5 min. After 3 times of washing, an aliquot of the final supernatant was saved for the background reading, before the resuspension of enteroid pellet. The fluorescent intensity of the final enteroid suspension was measured by a fluorescent plate reader under Excitation/Emission wavelength 485/528 nm. The intact enteroids number of each well was counted to normalize the FD4 fluorescence, as shown in the formula below.

$$\text{FD4 fluorescence} = \frac{\text{FD4 fluorescence intensity} - \text{Background}}{\text{Enteroid number}}$$

Enteroid glucose (2-NBDG) absorption analysis

2-(N-(7-Nitrobenz-2-oxa-1,3-diazol-4-yl)Amino)-2-Deoxyglucose (2-NBDG) (N13195, Invitrogen) was used for absorption analysis. Phlorizin (11576, Cayman), a sodium-glucose linked transporter (SGLT1) specific inhibitor, was used as a blockade for glucose active absorption. Briefly, enteroids were treated with or without 300 nM phlorizin at 37°C for an hour followed by treatment with 100 μM 2-NBDG at 37°C for 2 h. After treatment, the 2-NBDG residual in the medium was removed via ice-cold PBS wash, followed by 300 × *g* centrifugation at 4°C for 5 min. After 3 times of washing, an aliquot of the final supernatant was saved for the background reading, before the resuspension of enteroid pellet. The fluorescent intensity of the final enteroid suspension was measured by a fluorescent plate reader under Excitation/Emission wavelength 465/540 nm. The intact enteroid number of each well was counted to normalize the 2-NBDG fluorescence, as shown in the formula below.

$$\text{2NBDG fluorescence} = \frac{\text{2NBDG fluorescence intensity} - \text{Background}}{\text{Enteroid number}}$$

Ussing chamber analysis

Intestinal physiologic functions were evaluated by the Ussing chamber system. The Ussing chamber procedure was modified from previous studies [23]. Briefly, the middle ileum was cut open along the mesentery. The muscle layers of the intestine were stripped off in ice-cold and oxygenated Ringer's

TABLE 1
Primer sequence list for qRT-PCR

Gene	Forward	Reverse	Target	Gene name	Accession number
ChgA	AAGCCAACACTGATGAAGAAGG	CTGAGGTGAGTACTGGGAGC	Enteroendocrine cells	Chromogranin A	XM_015287755.2
MUC2	ATTGAAGCCAGCAATGGTGT	TTGTTGGCCTTGTCATCAAA	Goblet cells	Mucin 2	XM_046942297.1
LYZ	GACGATGTGAGCTGGCAG	GGATGTTGCACAGGTTCC	Paneth cells	Lysozyme	NM_205281
PCNA	GGCTTCGACACCTACCGCT	GAGCCAACGTATCCGCATTGT	Proliferation cells	Proliferating cell nuclear antigen	NM_204170.2
Lgr5	ACGTCTTGCAGGAAATGGCT	TTGGCATCCAGGCGTAGAG	IESC	Leucine-rich repeat containing G protein-coupled receptor 5	XM_425441.5
Olfm4	TGACAACGACAGACGTGACTC	AGAACTTTGGGGAGGTGTGC		Olfactomedin 4	NM_001040463.1
Dll1	GCTTCAATGGAGGGCGATGC	GAGTTCCCCAGGTCAACGCA	Secretory progenitors	Delta-like canonical Notch ligand 1	NM_204973.2
Hes1	TAGTTCGCGGCACTCCAAGC	ACTTGCCCAGCACCGTAGG	Absorptive progenitors	Hes family bHLH transcription factor 1	XM_015291592.2
ZO1	TGAAGGACCCCAGTGACACG	CACTCATGGCTGGGAGCGTA	Tight-junction proteins	Tight-junction protein 1	XM_015278981.2
ZO2	GCCCCAGCCAAAAGCAGTTA	CCAGCAAGTCGCAGACCAAC		Tight-junction protein 2	NM_204918.1
CLDN1	GCGGGGGACAACATCGTGAC	AGACCCAGGAGTATGGCGGC		Claudin 1	NM_001013611.2
CLDN2	GACGTGAACCATTCGCAGTCC	GTTTTGTGAGGGCACAGGCA		Claudin 2	NM_001277622.1
OCLN	CGCTACGGCAAAGCCAACAT	CCATCCGCCACGTTCTTCAC		Occludin	NM_205128.1
SGLT1	GCCATGGCCAGGGCTTA	CAATAACCTGATCTGTGCACCAGTA	Nutrient transporters	Solute carrier family 5 member 1	NM_001293240.2
GLUT2	ATGACGGTTGGACTTGTGCT	CAATGAAGTTGCAGGCCCAG		Solute carrier family 2 member 2	NM_207178.1
B0AT1	AGGTGGGAGGAGCGGAATTT	TGCGGGTGCTCTCATGTATT		Solute carrier family 6 member 19	XM_419056.6
EAAT3	TGCTGCTTTGGATTCCAGTGT	AGCATGACTGTAGTGCAGAAGTAATATAT		Solute carrier family 1	XM_424930.5
PepT1	AGACTGGGCAAGCGAGAAGT	TGCCCAGAACATCGGGAGAG		Solute carrier family 15 member 1	NM_204365.2
TBP	CTTCGTGCCCGAAATGCT	GCGCAGTAGTACGTGGTTCTCTT	Internal controls	TATA-box binding protein	NM_205103
RPL1	TCTCCACGACGACGAAGTCA	CCGCCGCCTTGATGAG		Ribosomal protein lateral stalk subunit P1	NM_205322.1
RPL4	TCAAGGCGCCCATTCG	TGCGCAGGTTGGTGTGAA		Ribosomal protein L4	NM_001007479.1

solution. A piece of 0.3–0.5-cm^2 mucosa was mounted on the Ussing chamber filled with Ringer's solution. A total of 10-mM glucose was added to the serosal side as tissue energy source, and 10 mM mannitol was added to the mucosal side for balancing osmotic pressure. A protease inhibitor cocktail (78425, Thermo Fisher Scientific) was added in the serosal side to prevent dipeptidyl peptidase IV degradation of enteroendocrine product. After mounting, tissues were allowed for a 20-min equilibration period, then the tissue was short-circuited by clamping the voltage to zero. The short-circuit current (*Isc*, $\mu A/cm^2$) and transepithelial resistance (TER, $\Omega \times cm^2$) were continuously recorded by the chamber software (Acquire and Analyze 2.3, Physiologic Instruments Inc.). For electrogenic nutrient transport measurement, a dose of 10-mM nutrients (glucose, di-peptide glycylsarcosine [G3127, Sigma], alanine, Gln, lysine) was added to the luminal side (osmotically balanced with 10-mM mannitol in serosal side), and changes in response to nutrients addition (delta *Isc*) was recorded and calculated. For permeability measurement, one dose of FD4 (1 mg/mL) was added to the luminal side, and FD4 leakage in the serosal chamber was quantified.

Statistical analysis

Data are expressed as the mean ± SEM from the indicated sample number. Statistical significance between 2 groups was analyzed by Student's *t*-test. Statistical significance between multiple groups was analyzed via one-way ANOVA followed by Tukey post hoc test. Analysis was performed using the SigmaPlot version 12 software. *P* values of ≤ 0.05 were considered statistically significant. *P* values of ≤ 0.01 were considered a trend of significance.

Results

Intestinal length and ileal morphology

Early life Gln supplementation significantly stimulated intestinal growth during the peri-hatch period. The in-ovo Gln injection at E18 significantly increased intestinal length (Figure 1A) on the day of hatch, in comparison with PBS injection control. In the ileum, the villus height and villus height: crypt depth ratio were significantly increased, whereas the crypt depth and crypt fission were not significantly changed in Gln-treated birds (Figure 1B).

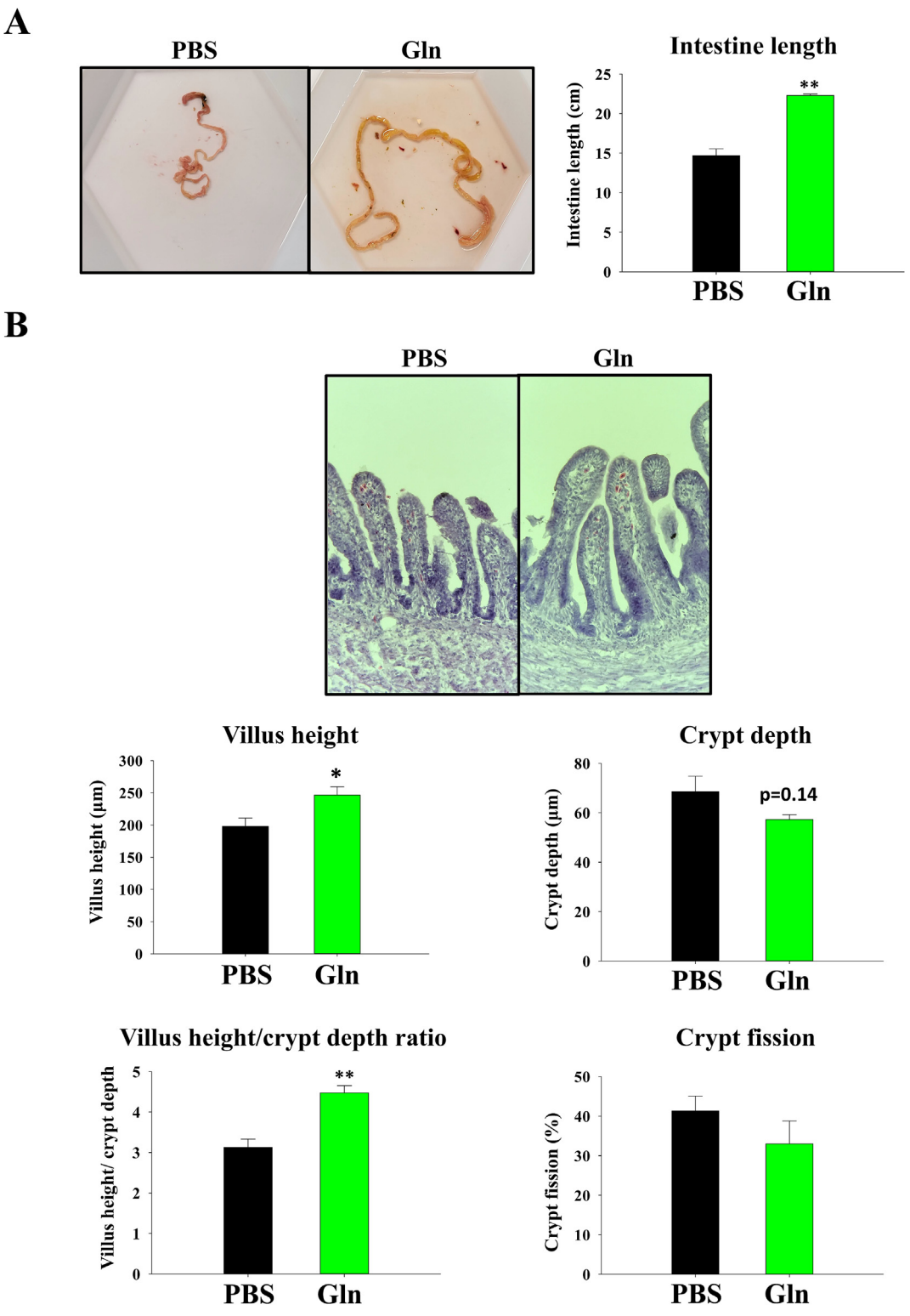

FIGURE 1. Effects of in-ovo glutamine (Gln) on small intestinal length and ileal morphology on the day of hatch. (A) Small intestinal length measurement after linearization. (B) Ileal tissue histologic measurements. Data are presented as the mean ± SEM from ≥6 embryos. *$P \leq 0.05$; **$P \leq 0.01$.

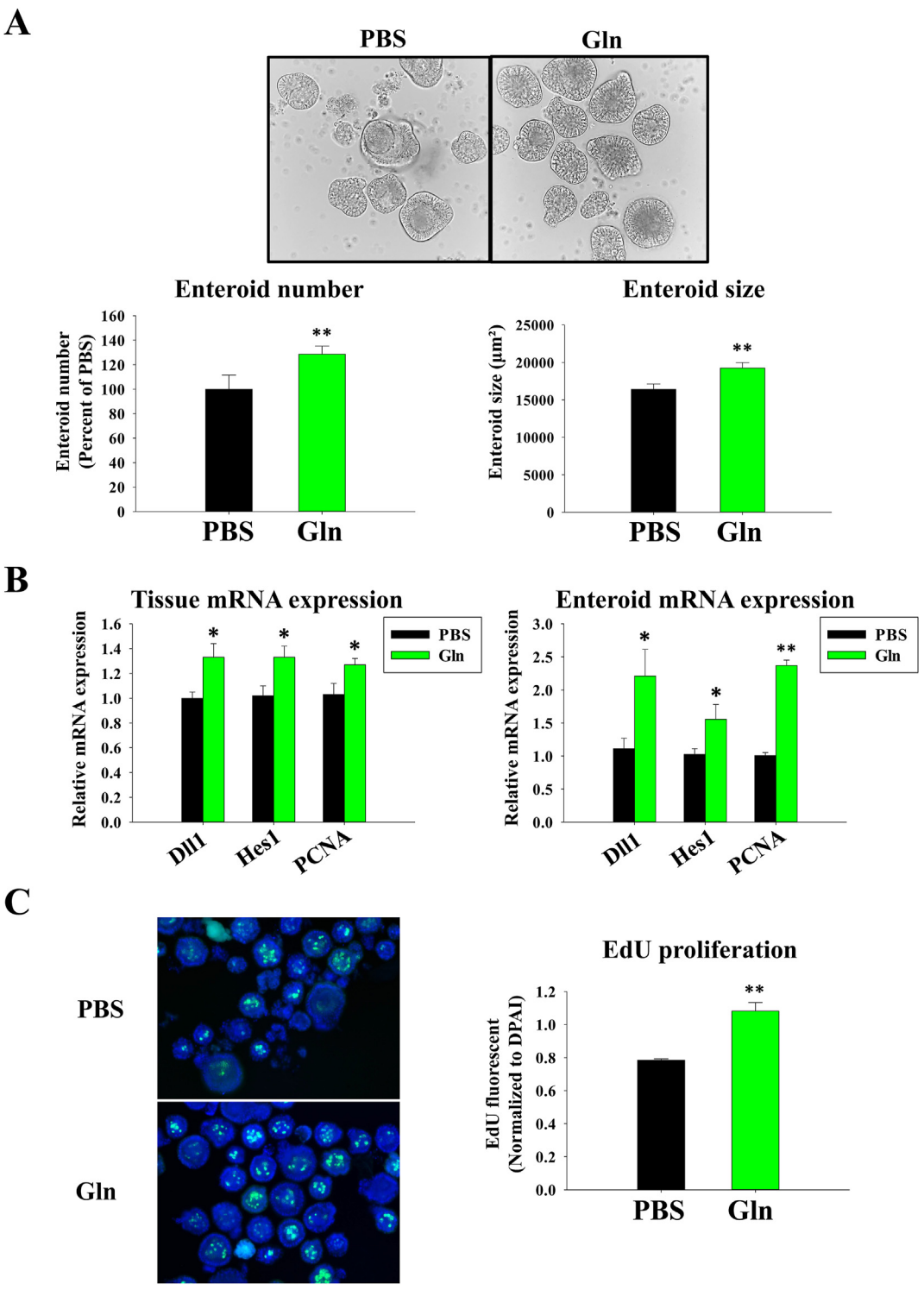

FIGURE 2. Effects of in-ovo (Gln) on the proliferation and differentiation of intestinal epithelial stem cells (IESC) in ileal tissue and enteroids on the day of hatch. (A) The number and size of apical-out enteroids isolated from the small intestine and cultured for 4 d. (B) The mRNA expression of differentiation and proliferation markers in ileum tissue and enteroids. (C) 5-ethynyl-2′-deoxyuridine (EdU)cell proliferation assay in the enteroids; Blue fluorescent: 4′,6-diamidino-2-phenylindole (DAPI) (nuclei); Green fluorescent: EdU (proliferate cells). Data are presented as the mean ± SEM from ≥6 embryos. *$P \leq 0.05$; **$P \leq 0.01$.

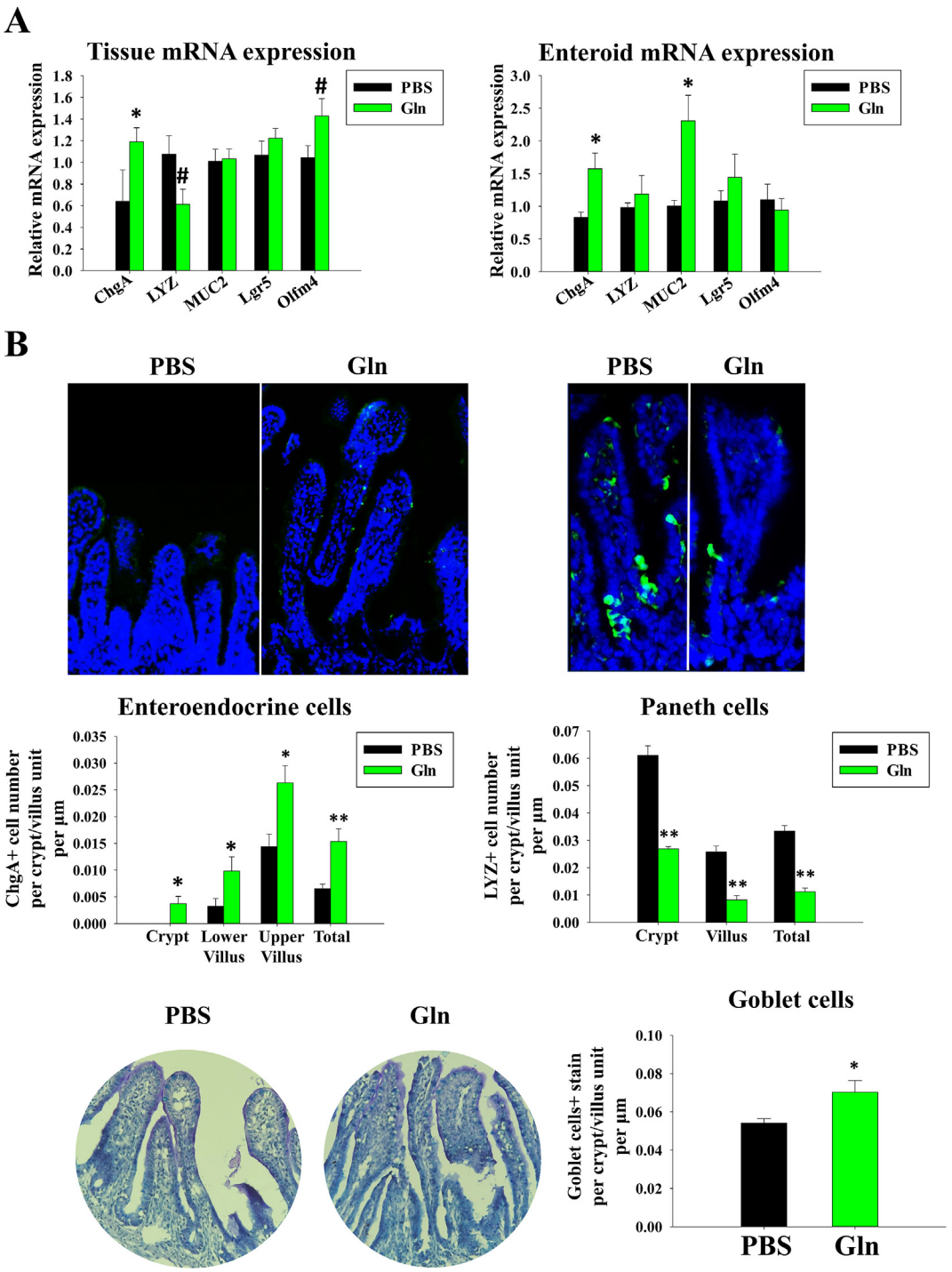

FIGURE 3. Effects of in-ovo Gln on ileum epithelial cell population on the day of hatch. (A) The marker genes mRNA expression of epithelial cells in the ileum tissue and enteroids. (B) Immunofluorescent staining [ChgA for Enteroendocrine cells (EEC), LYZ for Paneth cells] and Alcian-Blue periodic acid-Schiff (PAS) staining (goblet cells) in the ileum. In EECs images (left), blue fluorescent: 4′,6-diamidino-2-phenylindole (DAPI) (nuclei); Green fluorescent: Chromogranin A (ChgA). In Paneth cells images (right), blue fluorescent: DAPI (nuclei); Green fluorescent: Lysozyme (LYZ). Data are presented as the mean ± SEM from ≥6 embryos. $^{\#}0.05 < P \leq 0.1$; $^{*}P \leq 0.05$; $^{**}P \leq 0.01$.

Intestinal epithelial proliferation and differentiation potential

To evaluate whether in-ovo Gln influenced epithelial cell activities, the ileal tissue and the apical-out enteroids isolated from ileal villus units at hatch time were analyzed. After 2 d of culture, enteroids were formed from epithelial villus units (Supplemental Figure 1). In-ovo Gln feeding significantly increased enteroid number and size, as well as the EdU positive-stained cell numbers (Figure 2A and C), as indications of accelerated epithelial proliferation. Furthermore, PCNA (proliferating cell marker) mRNA expressions were significantly increased in both ileum tissue and apical-out enteroids. Interestingly, the mRNA expressions of both Dll1 (secretory cell precursor marker) and Hes1 (absorptive cell precursor marker) were significantly increased in the ileal tissue and enteroids (Figure 2B).

Intestinal epithelial cell composition

We further evaluated how in-ovo Gln affected IESC and secretory cell populations. mRNA expressions of Olfm4 (active stem cell marker) but not Lgr5 tended to be increased in ileum on the day of hatch (Figure 3A). In the ileal tissue, the number and density of ChgA positive-stained cells (EEC) and Alcian-Blue–PAS positive cells (goblet cells) were significantly increased, whereas the number and density of LYZ positive-stained cells were significantly decreased (Figure 3B). At the molecular level, mRNA expression of ChgA was significantly increased, whereas LYZ (Paneth cell marker) was decreased (Figure 3A). In the apical-out enteroids, gene expressions of ChgA (EEC marker) and MUC2 (goblet cell marker) were both increased significantly. These data suggest that all epithelial secretory cell differentiations were enhanced by Gln, except for the Paneth cell population.

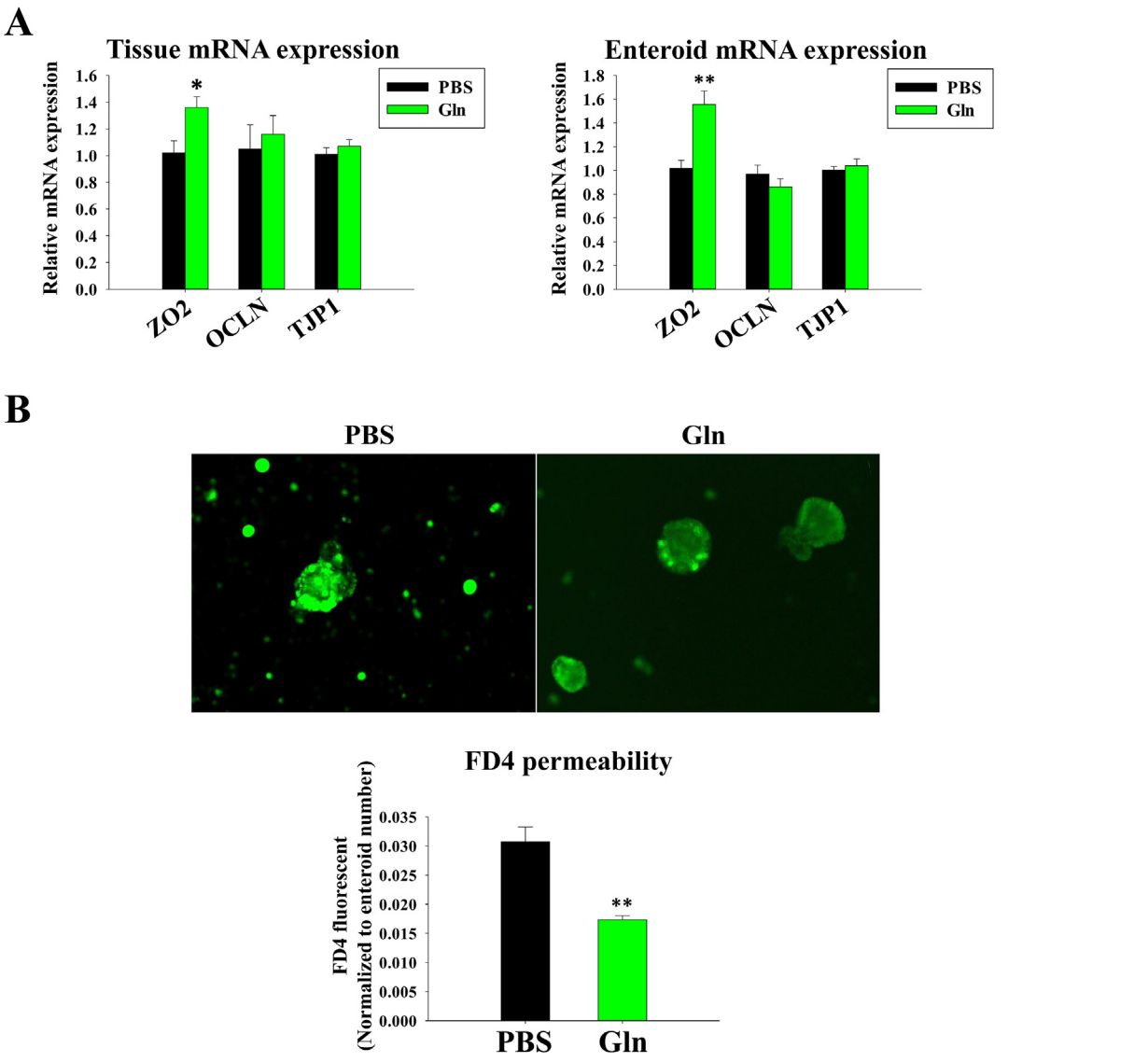

FIGURE 4. Effects of in-ovo Gln on epithelial tight-junction's gene expression and barrier function in the ileum and enteroids on the day of hatch. (A) The mRNA expressions of intestinal tight-junction proteins in the ileum tissue and enteroids. (B) FD4 permeability analysis in apical-out enteroids after 4 d in culture. Green fluorescent: FD4. Data are presented as the mean ± SEM from ≥6 embryos. *$P \leq 0.05$; **$P \leq 0.01$. FD4, fluorescein isothiocyanate-4 kDa dextran.

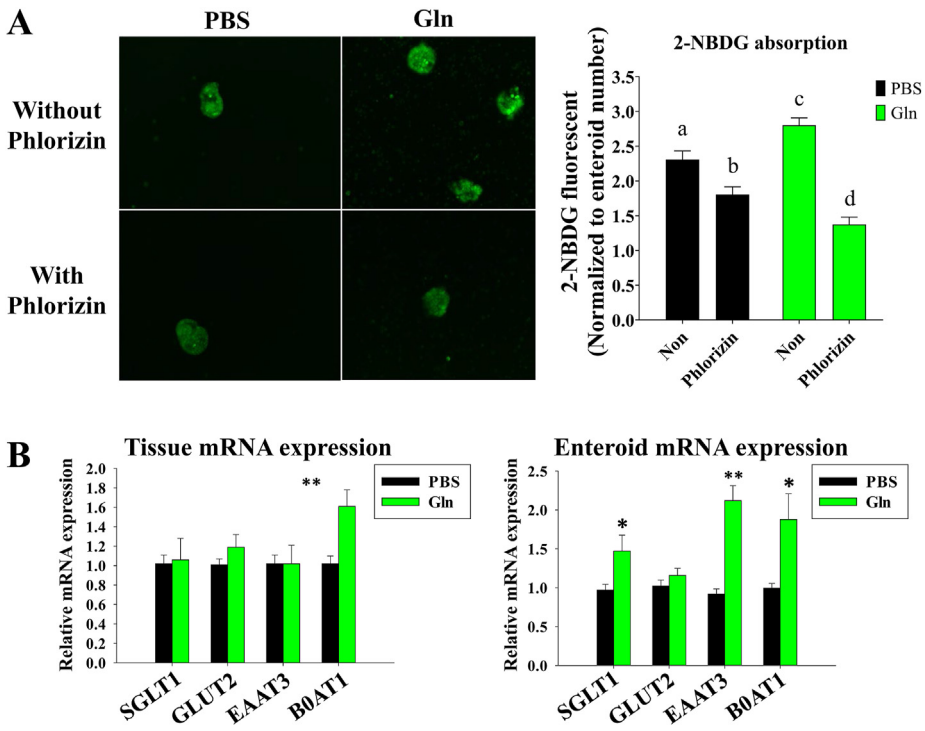

FIGURE 5. Effects of in-ovo Gln on intestinal nutrient transporters gene expression and glucose absorptive function in the ileum and enteroids on the day of hatch. (A) 2-NBDG absorption analysis in the enteroids after 4 d in culture. Green fluorescent: 2-NBDG. (B) The mRNA expressions of intestinal nutrient transporters in the ileum tissue and enteroids. Data are presented as the mean ± SEM from ≥6 embryos. $^{*}P \leq 0.05$; $^{**}P \leq 0.01$ compared between Gln and PBS groups. Different letters indicate $P \leq 0.05$ among treatments. 2-NBDG, 2-(N-(7-Nitrobenz-2-oxa-1,3-diazol-4-yl) Amino)-2-Deoxyglucose.

Intestinal epithelial cell barrier and absorptive functions on the day of hatch

To examine the immediate effects of in-ovo Gln on intestinal functions at hatch, gene expression and functional assays in apical-out enteroids were used. In the enteroids that were isolated from Gln-treated embryos, the gene expression of tight-junction protein (ZO2) was increased in both enteroids and intestinal tissue (Figure 4A). The paracellular permeable FD4 was significantly reduced (Figure 4B). The total absorption of NBD-labeled glucose increased in enteroids from in-ovo Gln birds compared with in-ovo PBS birds (Figure 5A).

To further specify this increase in glucose transport originating from SGLT1 functions, enteroids were pretreated with phlorizin (an SGLT1-specific blocker) before glucose addition. The total glucose transport was significantly blocked in both the PBS-phlorizin group and the Gln-phlorizin group. After the phlorizin treatment, the paracellular and passive (GLUT2 mediated) glucose transport were significantly lower in enteroids from in-ovo Gln birds compared with in-ovo PBS birds (Figure 5A). Given the reduced paracellular FD4 permeability result observed above, this enhanced 2-NBDG transport was more likely via SGLT1 activities than paracellular glucose diffusion. In enteroids, the mRNA expressions of SGLT1 (glucose transporter), EAAT3 (anion AA transporter), and B0AT1 (neutral AA transporter) were upregulated in the in-ovo Gln bird. In the ileal tissue, only B0AT1 mRNA expression was increased (Figure 5B). The data from both enteroids and intestinal tissues on the day of hatch suggested an increased nutrient transport functions immediately following Gln in-ovo nutrition.

BW and intestinal barrier and absorptive functions at posthatch period

The BW of birds treated with in-ovo Gln tended to increase at d3 but showed no difference at d7 and d14 (Figure 6A). To evaluate whether early in-ovo Gln introduced long-term changes in intestinal functions in later life, Ussing chamber electrophysiologic analyses were used on the ileal tissue at d3 and d14 posthatch. At d3, the basal *Isc* (ion secretion indicator), TER (epithelial integrity indicator), and FD4 permeability were not changed in treated birds (Figure 6B). Alanine transport tended ($P < 0.1$) to increase in the in-ovo Gln group at d3 (Figure 6C). At d14 posthatch, in-ovo Gln significantly increased electrogenic transports of di-peptide and alanine in the ileum (Figure 6C). Interestingly, FD4 permeability tended to increase in the Gln group. These results indicated a long-term beneficial effect of in-ovo Gln injection on later posthatch gut nutrient transport functions.

Discussion

In this study, the short- and long-term effects of early life nutrition via in-ovo Gln supplementation at E18 were evaluated in broiler chickens. The embryos were allowed for 3 d of nutritional stimulation. On the day of hatch, significant improvement

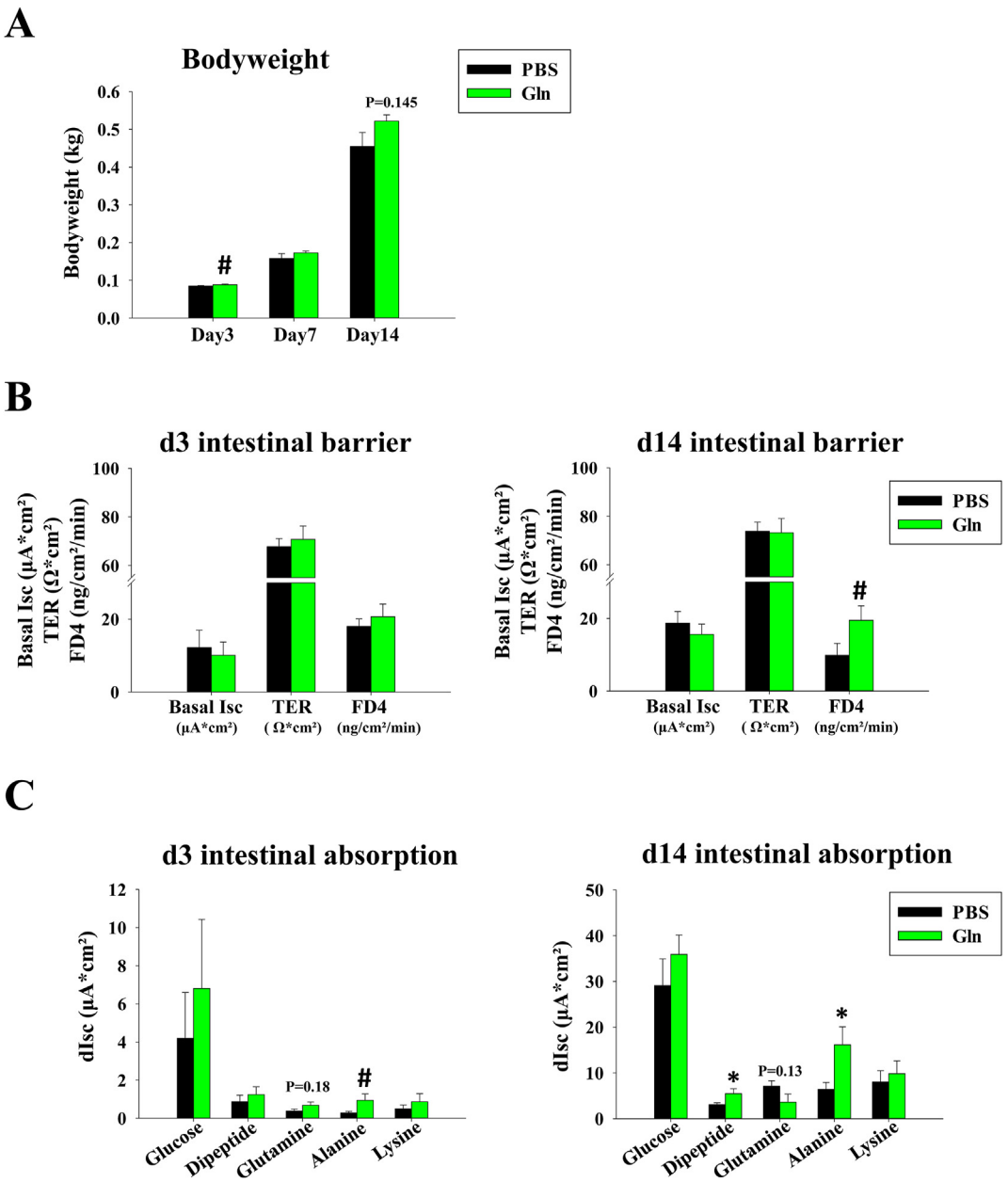

FIGURE 6. The effects of in-ovo Gln on growth performance, intestinal barrier, and nutrient absorption functions in the ileum at day 3 and day 14 posthatch. (A) Body weight of chickens posthatch. (B) Ileum barrier functions are indicated by the Ussing chamber measurements of the basal *I*sc, TER, and FD4. (C) Ileum electrogenic nutrient absorptive functions are indicated by Ussing chamber measurements of the d*I*sc for glucose, dipeptide (Gly-Sar), glutamine, alanine, and lysine. Data are presented as the mean ± SEM from ≥4 chickens. $^{\#}0.05 < P \leq 0.1$; $^{*}P \leq 0.05$; $^{**}P \leq 0.01$ comparing between Gln and PBS. Basal *I*sc, basal short-circuit current; TER, transepithelial electrical resistance; FD4, fluorescein isothiocyanate-4 kDa dextran; d*I*sc, delta short-circuit current change in response to the nutrient addition.

in small intestinal growth and maturation were indicated by intestinal length and mucosa morphologic measurements. Similar results have been observed in other groups. Sözcü and Ak [24] reported that in-ovo injection of Gln increased small intestinal length by ~45% at hatch. In addition, the villus height and villus to crypt ratio were increased on the day of hatch by in-ovo injection of Gln [18], threonine (Thr) [25], or arginine [26]. In fact, early life nutrition programming (including in-ovo nutrition and posthatch feeding) has been suggested as a strategy to modulate intestinal development in poultry (reviewed, [4]).

As a complicated and dynamically regulated organ, the intestinal functions are tightly associated with epithelial cell composition and homeostasis but are not always in line with structural or histologic features of the mucosa [27,28]. However, few studies evaluated the intestinal functions of in-ovo Gln. In this repeatable model of early-nutrition-stimulated intestinal maturation, we further investigated intestinal epithelial cell composition and their basic intestinal functions posthatch.

Intestinal epithelial cells go through dramatic proliferation and maturation during peri-hatch periods [29]. Such rapid growth and expansion rely on IESCs activities, including active self-proliferation and generation of absorptive and secretory precursor cells, which eventually differentiate into functional mature cells [30]. It is not convenient to analyze epithelial

proliferation and differentiation activities in vivo. Therefore, a recently established technique for generating chicken enteroids was utilized in this study. These 3D enteroids consist of all types of epithelial cells, encapsulating the core lamina propria cells and immune cells which closely recapitulate intestinal villus properties [16]. Their apical-out feature allows easy access to their luminal side for evaluating epithelial functions; these primary cultures also reflect any host-specific tissue programming effects.

Our enteroid culture results showed that the enteroids isolated from in-ovo Gln-treated intestines were not only more in number but also greater in size (Figure 2A). Given the fact that these enteroids were formed by epithelial cell encapsulation (epithelial wound healing), our data suggested that in-ovo Gln treatment might enhance epithelial regeneration capability and proliferation rate. The programming effect of enhanced proliferation was further confirmed in the in vitro EdU proliferating assay when intestinal cells were cultured in days out of the embryo (Figure 2C). Other groups also reported enhanced cell proliferation effects by in-ovo Gln (Sox9 stained cells [18]). In our study, at the molecular level, Gln treatment simultaneously upregulated cell proliferation gene marker (PCNA), epithelial-specific gene marker for absorptive precursor cells (Hes1) and secretory precursor cells (Dll1) [14,31]. Interestingly, these findings showed similar trends both in ileal gut tissues and in the isolated enteroids. However, discrepancies between tissue and enteroids were observed in terms of MUC2, SGLT1, and EAAT3 mRNA expression. This might be because apical-out enteroids were derived from the upper villus area of the epithelium and were less representative of the crypt regions. Therefore, the Gln effects on the intestinal villus could be more readily observed in the enteroids than in the tissue samples. Overall, our data supported that the apical-out enteroid model closely recapitulated in vivo intestinal villus features [16,32].

Considering the potentially underrepresented crypt cell population in enteroids, we further evaluated the downstream secretory cell lineage allocations to EECs, Paneth cells, and goblet cells mostly in the intestinal tissues. Surprisingly, we found significant repression of Paneth cell number, but a significant increase in EEC and goblet cell number (Figure 3). In mammalian animals, Paneth cells are located in the crypt region and support the stem cell niche environment [33,34]. It is worth noting that Paneth cells in chickens might be located throughout the whole crypt/villus axis [35,36]. Although an unknown mechanism, such decreasing of Paneth cells had been previously found in early life intestinal development in chicken, including duodenum, jejunum, and ileum segments [37,38]. Few researchers studied early life nutrition and EEC development and functions. It is known that glucagon-like peptide 2 secreted by EECs increased IESC proliferation [39] and intestinal development [40–43]. A recent publication studying in-ovo Gln reported significant increases in intestinal GLP-2R, insulin-like growth factor 1, and insulin-like growth factor 1 receptor gene expression before and after hatch, which is in line with our findings [44]. Therefore, instead of Paneth cells, the upregulated EEC in our study might be the underlying mechanism by which one-time in-ovo Gln supplement enhanced proliferation and differentiation of the intestine posthatch. There are contradictory reports about in-ovo nutritional stimulation influencing goblet cell numbers. Previous studies showed that in-ovo Gln did not change goblet cell number at hatch [18], but that in-ovo Thr increased ileal MUC2 at hatch [25]. Further investigations are needed to resolve these controversies.

We finally evaluated the function of intestinal absorptive cells (enterocytes), in terms of nutrient transport and barrier permeability with or without in-ovo Gln stimulation. With the aforementioned similarity between intestinal tissue and enteroids, we were able to use enteroids to mimic intestinal tissue functions on the day of hatch. In terms of glucose absorption, the transporter SGLT1 is located at the apical membrane, whereas GLUT2 is mainly present at the basolateral membrane, but can be recruited to the apical membrane when sugar level in the intestine is elevated. We found that both paracellular barrier functions and SGLT1-mediated active glucose transport functions were upregulated on the day of hatch. The reduced FD4 permeability could have originated from upregulation in tight-junction protein (ZO2, Figure 4), whereas the increased glucose transport could be contributed by a higher number of SGLT1 transporter (Figure 5). Such increases in apical transporter SGLT1 would result in the transport of sugars from the lumen into the enterocytes. Although we did not measure amino acid transport functions in enteroids, the upregulated EAAT3 and B0AT1 transporter gene expressions might be an estimation of increased absorptive function. Our data also suggested that the apical-out primary enteroids culture would be an ideal alternative method to evaluate the embryonic intestinal functions in vitro.

At d3 and d14 posthatch, we evaluated the long-term effects of in-ovo Gln on intestinal absorptive and barrier functions by using Ussing chambers. For glucose transport, the gene expression of SGLT1 and electrogenic glucose transport (mediated by SGLT1) were not significantly changed. This differs from the above-mentioned enteroid results on the day of hatch. It is possible that other nonepithelial regulatory mechanisms, such as the enteric nervous system and immune cells, may have interfered with the tissue measurements but not in enteroids. In addition, it remains unclear whether the enhanced SGLT1 glucose transport induced by in-ovo Gln can be compensated for through posthatch feeding. Future research is needed to fully understand this aspect. Interestingly, the expression of GLUT2 was upregulated at d14 posthatch (Supplemental Figure 2B). As discussed above, such upregulation in basolateral GLUT2 would facilitate apical glucose transport via GLUT2 apical translocation, and also contribute to the basolateral transport of sugars out of the enterocytes. For amino acids transport, no difference was observed in lysine (cationic amino acid) or Gln (neutral amino acid) transport. However, the transport of another neutral amino acid (alanine) was consistently upregulated at d3 (trend) and d14 posthatch. Little is known about the mechanism specifically regulating transport of individual neutral amino acids. In the rabbit gut inflammation model, previous research discussed unique inhibition patterns of Na-Gln co-transporter (B0AT1) and Na-alanine co-transporter [amino acid transporter B0 (ATB0)] via regulating numbers of transporter or substrate affinity of transporter, respectively [45]. Because multiple transporters (such as B0AT1, alanine serine cysteine transporter1, ATB0, etc.) control intestinal neutral amino acids transport, and the tissue demand for each amino acid may be dynamically altered during the growing of chickens [46], future studies are needed to fully understand the effects of in-ovo Gln on these aspects. In addition, the electrogenic transport of di-peptide [mediated by peptide transporter 1

(PepT1)] was significantly increased at d14 posthatch, which was in line with a tendency of upregulated PepT1 gene expression (Supplemental Figure 2B). Although the increases of electrogenic transport and gene expression may not reflect the total nutrient absorption, this consistent increase in nutrient transporter function and gene expression suggested that in-ovo Gln feeding was sufficient to increase the intestinal absorption in the long term. Indeed, recent studies showed that in-ovo nutrients (amino acid or carbohydrate) feeding increased disaccharidase activities, SGLT1 and GLUT2 gene expression in geese [8,47,48], and SGLT1 and PepT1 in broilers [44]. On the other hand, no significant difference was observed in the ileal barrier function at d3. Surprisingly, the paracellular FD4 permeability tended to increase at d14 in the in-ovo Gln birds. Furthermore, the gene expression of tight-junction proteins, claudin 1 (CLDN1) and OCLN, were downregulated (Supplemental Figure 2C). It has been well documented by other groups that in-ovo Gln enhanced intestinal morphology and cell proliferation peri-hatch and posthatch [18,47,49]. However, few papers measured the gut permeability at later life following early life in-ovo stimulation. It is possible that intestinal barrier functions are not tightly associated with mucosal structure and histology [27,28]. Considering the remodeling of tight-junction protein during epithelial cell anoikis, the rapid proliferation and turnover rate may induce persorption and dynamically increased permeability [18,50]. In a recent paper of in-ovo Gln in chickens, enhanced tight-junction expressions (TJP-2 and Occludin) were fading at d7 compared with d3 posthatch; however, the beneficial effects on nutrient transporter expression (SGLT1 and PepT1) were sustained during growth [44]. This decline of posthatch barrier function of in-ovo Gln and the underlying mechanism require further studies' confirmation. The overall enhanced nutrient transport function was consistent among studies. In addition, the increased intestinal permeability may lead to increased nutrient absorption via paracellular absorption [51,52]. Such compromised barrier and enhanced nutrient transport may be beneficial in the health conditions but could be detrimental to intestinal health under challenging environments. Future studies are needed to fully understand long-term functional changes after early life in-ovo Gln supplementation and combination with disease circumstances, especially on the aspects of intestinal absorption and permeability.

In summary, this study demonstrated a combination of in-ovo nutrient administration, apical-out enteroids, and novel intestinal functional analysis methods. Furthermore, this study indicated in-ovo Gln feeding on day 18 chicken embryo increased intestinal development in day 21 embryos, including increased intestinal morphogenesis, cell proliferation, differentiation, and intestinal functional maturation. The in-ovo Gln feeding showed a high potential to be utilized to increase intestinal development before hatching for preparing rapid growth after hatching. The novel analysis methods for chicken intestinal function are sufficient tools for different quantification of treatments.

Acknowledgments

We thank Dr Mark Parcells at the Department of Animal and Food Sciences at the University of Delaware for the technical training and support of in-ovo injection.

Author contributions

The authors' responsibilities were as follows – LY: designed and conducted in-ovo injection, animal feeding, sample analysis, and enteroid experiments, performed data analysis, and manuscript writing; PM, LS: were involved in animal feeding, sampling, and Ussing chamber experiments; PM, FG: were involved in troubleshooting of enteroids experiments; MS, AH: contributed to RT-PCR experiments; YL: conceptualized the study, designed the experiments, and was also involved in Ussing chamber experiments, data analysis, and the writing of manuscript; and all authors: read and approved the final manuscript.

Conflict of interest

The authors report no conflicts of interest.

Funding

This work was supported by startup funding (ANSC195174) from the College of Agricultural and Natural Resources at the University of Delaware.

Data availability

All the data supporting the finding are available within the article and its supplementary materials. Raw data that supports the findings of this study are available from the corresponding author, upon reasonable request.

Appendix A. Supplementary data

Supplementary data to this article can be found online at https://doi.org/10.1016/j.tjnut.2024.02.007.

References

[1] G.B. Havenstein, P.R. Ferket, M.A. Qureshi, Growth, livability, and feed conversion of 1957 versus 2001 broilers when fed representative 1957 and 2001 broiler diets, Poult. Sci. 82 (2003) 1500–1508, https://doi.org/10.1093/ps/82.10.1500.

[2] Z. Uni, E. Tako, O. Gal-Garber, D. Sklan, Morphological, molecular, and functional changes in the chicken small intestine of the late-term embryo, Poult. Sci. 82 (2003) 1747–1754, https://doi.org/10.1093/ps/82.11.1747.

[3] Y. Dror, I. Nir, Z. Nitsan, The relative growth of internal organs in light and heavy breeds, Br. Poult. Sci. 18 (1977) 493–496, https://doi.org/10.1080/00071667708416389.

[4] R. Jha, A.K. Singh, S. Yadav, J.F.D. Berrocoso, B. Mishra, Early nutrition programming (in ovo and post-hatch feeding) as a strategy to modulate gut health of poultry, Front. Vet. Sci. 6 (2019) 82, https://doi.org/10.3389/fvets.2019.00082.

[5] X.Y. Dong, Y.M. Wang, H.H. Song, X.T. Zou, Effects of in ovo injection of carbohydrate solution on small intestine development in domestic pigeons (Columba Livia), J. Anim. Sci. 91 (2013) 3742–3749, https://doi.org/10.2527/jas.2013-6400.

[6] S.L. Cheled-Shoval, E. Amit-Romach, M. Barbakov, Z. Uni, The effect of in ovo administration of mannan oligosaccharide on small intestine development during the pre- and posthatch periods in chickens, Poult. Sci. 90 (2011) 2301–2310, https://doi.org/10.3382/ps.2011-01488.

[7] S.B. Yang, Y.J. Qin, X. Ma, W.M. Luan, P. Sun, A.Q. Ju, et al., Effects of in ovo injection of astragalus polysaccharide on the intestinal development and mucosal immunity in broiler chickens, Front. Vet. Sci. 8 (2021) 738816, https://doi.org/10.3389/fvets.2021.738816.

[8] X. Dang, H. Zhou, Y. Lou, D. Li, Effects of in ovo feeding of methionine and/or disaccharide on post-hatching breast development, glycogen reserves, nutrients absorption parameters, and jejunum antioxidant

indices in geese, Front. Vet. Sci. 9 (2022) 944063, https://doi.org/10.3389/fvets.2022.944063.
[9] M.J. Chen, J.Y. Zhou, Y.J. Chen, X.Q. Wang, H.C. Yan, C.Q. Gao, The in ovo injection of methionine improves intestinal cell proliferation and differentiation in chick embryos by activating the JAK2/STAT3 signaling pathway, Anim. Nutr. 7 (2021) 1031–1038, https://doi.org/10.1016/j.aninu.2021.03.009.
[10] W. Chen, R. Wang, X.L. Xiong, H.F. Wan, J. Xu, J. Peng, Influence of in ovo injection of disaccharides, glutamine and beta-hydroxy-beta-methylbutyrate on the development of small intestine in duck embryos and neonates, Br. Poult. Sci. 51 (2010) 592–601, https://doi.org/10.1080/00071668.2010.520533.
[11] B.C. Peck, A.T. Mah, W.A. Pitman, S. Ding, P.K. Lund, P. Sethupathy, Functional transcriptomics in diverse intestinal epithelial cell types reveals robust microrna sensitivity in intestinal stem cells to microbial status, J. Biol. Chem. 292 (2017) 2586–2600, https://doi.org/10.1074/jbc.M116.770099.
[12] E.C. Moorefield, S.F. Andres, R.E. Blue, L. Van Landeghem, A.T. Mah, M.A. Santoro, et al., Aging effects on intestinal homeostasis associated with expansion and dysfunction of intestinal epithelial stem cells, Aging (Albany NY) 9 (2017) 1898–1915, https://doi.org/10.18632/aging.101279.
[13] D. Zeve, E. Stas, J. de Sousa Casal, P. Mannam, W. Qi, X. Yin, et al., Robust differentiation of human enteroendocrine cells from intestinal stem cells, Nat. Commun. 13 (2022) 261, https://doi.org/10.1038/s41467-021-27901-5.
[14] J.H. van Es, T. Sato, M. van de Wetering, A. Lyubimova, A.N. Yee Nee, A. Gregorieff, et al., Dll1+ secretory progenitor cells revert to stem cells upon crypt damage, Nat. Cell Biol. 14 (2012) 1099–1104, https://doi.org/10.1038/ncb2581.
[15] K. Kishida, S.C. Pearce, S. Yu, N. Gao, R.P. Ferraris, Nutrient sensing by absorptive and secretory progenies of small intestinal stem cells, Am. J. Physiol. Gastrointest. Liver Physiol. 312 (2017) G592–G605, https://doi.org/10.1152/ajpgi.00416.2016.
[16] T.J. Nash, K.M. Morris, N.A. Mabbott, L. Vervelde, Inside-out chicken enteroids with leukocyte component as a model to study host-pathogen interactions, Commun. Biol. 4 (2021) 377, https://doi.org/10.1038/s42003-021-01901-z.
[17] M.H. Kim, H. Kim, The roles of glutamine in the intestine and its implication in intestinal diseases, Int. J. Mol. Sci. 18 (2017) 1051, https://doi.org/10.3390/ijms18051051.
[18] N. Reicher, T. Melkman-Zehavi, J. Dayan, E.A. Wong, Z. Uni, Nutritional stimulation by in-ovo feeding modulates cellular proliferation and differentiation in the small intestinal epithelium of chicks, Anim. Nutr. 8 (2022) 91–101, https://doi.org/10.1016/j.aninu.2021.06.010.
[19] I. van der Wagt, I.C. de Jong, M.A. Mitchell, R. Molenaar, H. van den Brand, A review on yolk sac utilization in poultry, Poult. Sci. 99 (2020) 2162–2175, https://doi.org/10.1016/j.psj.2019.11.041.
[20] F.D. Wilson, T.S. Cummings, T.M. Barbosa, C.J. Williams, P.D. Gerard, E.D. Peebles, Comparison of two methods for determination of intestinal villus to crypt ratios and documentation of early age-associated ratio changes in broiler chickens, Poult. Sci. 97 (2018) 1757–1761, https://doi.org/10.3382/ps/pex349.
[21] Z.M. Dudhwala, P.D. Hammond, G.S. Howarth, A.G. Cummins, Intestinal stem cells promote crypt fission during postnatal growth of the small intestine, BMJ Open Gastroenterol 7 (2020) e000388, https://doi.org/10.1136/bmjgast-2020-000388.
[22] F. Ghiselli, L.E. Yu, A. Piva, E. Grilli, Y. Li, Evaluating protective effects of botanicals under inflammation and oxidative stress in chicken apical-out enteroids, Poult. Sci. 102 (2023) 102821, https://doi.org/10.1016/j.psj.2023.102821.
[23] S. Bialkowski, A. Toschi, L.E. Yu, L. Schlitzkus, P. Mann, E. Grilli, et al., Effects of microencapsulated blend of organic acids and botanicals on growth performance, intestinal barrier function, inflammatory cytokines, and endocannabinoid system gene expression in broiler chickens, Poult. Sci. 102 (2023) 102460, https://doi.org/10.1016/j.psj.2022.102460.
[24] A. Sözcü, İ. Ak, Effects of in-ovo injection of glutamine on late-term embryo development, hatchability, one-day old chick quality and small intestine morphological traits in broilers, Europ. Poult. Sci. 84 (2020), https://doi.org/10.1399/eps.2020.293.
[25] A.L.B. Moreira Filho, P.R. Ferket, R.D. Malheiros, C.J.B. Oliveira, P.C. Aristimunha, D.E. Wilsmann, et al., Enrichment of the amnion with threonine in chicken embryos affects the small intestine development, ileal gene expression and performance of broilers between 1 and 21 days of age, Poult. Sci. 98 (2019) 1363–1370, https://doi.org/10.3382/ps/pey461.
[26] T. Gao, M. Zhao, L. Zhang, J. Li, L. Yu, F. Gao, et al., ovo feeding of l-arginine regulates intestinal barrier functions of posthatch broilers by activating the mTOR signaling pathway, J. Sci. Food Agric. 98 (2018) 1416–1425, https://doi.org/10.1002/jsfa.8609.
[27] Q.J. Wu, N. Liu, X.H. Wu, G.Y. Wang, L. Lin, Glutamine alleviates heat stress-induced impairment of intestinal morphology, intestinal inflammatory response, and barrier integrity in broilers, Poult. Sci. 97 (2018) 2675–2683, https://doi.org/10.3382/ps/pey123.
[28] Y. Li, Z. Song, K.A. Kerr, A.J. Moeser, Chronic social stress in pigs impairs intestinal barrier and nutrient transporter function, and alters neuro-immune mediator and receptor expression, PLOS ONE 12 (2017) e0171617, https://doi.org/10.1371/journal.pone.0171617.
[29] N. Reicher, Z. Uni, Intestinal brush border assembly during the peri-hatch period and its contribution to surface area expansion, Poult. Sci. 100 (2021) 101401, https://doi.org/10.1016/j.psj.2021.101401.
[30] S. Umar, Intestinal stem cells, Curr. Gastroenterol. Rep. 12 (2010) 340–348, https://doi.org/10.1007/s11894-010-0130-3.
[31] V. Zecchini, R. Domaschenz, D. Winton, P. Jones, Notch signaling regulates the differentiation of post-mitotic intestinal epithelial cells, Genes Dev 19 (2005) 1686–1691, https://doi.org/10.1101/gad.341705.
[32] T.J. Nash, K.M. Morris, N.A. Mabbott, L. Vervelde, Temporal transcriptome profiling of floating apical out chicken enteroids suggest stability and reproducibility, Vet. Res. 54 (2023) 12, https://doi.org/10.1186/s13567-023-01144-2.
[33] H. Cheng, C.P. Leblond, Origin, differentiation and renewal of the four main epithelial cell types in the mouse small intestine. V. Unitarian theory of the origin of the four epithelial cell types, Am. J. Anat. 141 (1974) 537–561, https://doi.org/10.1002/aja.1001410407.
[34] J.C. Jones, C.D. Brindley, N.H. Elder, M.G. Myers, M.W. Rajala, C.M. Dekaney, et al., Cellular plasticity of defa4Cre-expressing Paneth cells in response to notch activation and intestinal injury, Cell. Mol. Gastroenterol. Hepatol. 7 (2019) 533–554, https://doi.org/10.1016/j.jcmgh.2018.11.004.
[35] Z. Uni R. Platin, D. Sklan, Cell proliferation in chicken intestinal epithelium occurs both in the crypt and along the villus, J. Comp. Physiol. B. 168 (1998) 241–247, https://doi.org/10.1007/s003600050142.
[36] E. Bar Shira, A. Friedman, Innate immune functions of avian intestinal epithelial cells: response to bacterial stimuli and localization of responding cells in the developing avian digestive tract, PLOS ONE 13 (2018) e0200393, https://doi.org/10.1371/journal.pone.0200393.
[37] C.J. Nile, C.L. Townes, G. Michailidis, B.H. Hirst, J. Hall, Identification of chicken lysozyme g2 and its expression in the intestine, Cell Mol. Life Sci. 61 (2004) 2760–2766, https://doi.org/10.1007/s00018-004-4345-z.
[38] L. Wang, J. Li, J. Li, R.X. Li, C.F. Lv, S. Li, et al., Identification of the Paneth cells in chicken small intestine, Poult. Sci. 95 (2016) 1631–1635, https://doi.org/10.3382/ps/pew079.
[39] M.E. Chen, S.M. Naeini, A. Srikrishnaraj, D.J. Drucker, Z. Fesler, P.L. Brubaker, Glucagon-like peptide-2 stimulates s-phase entry of intestinal Lgr5+ stem cells, Cell Mol. Gastroenterol. Hepatol. 13 (2022) 1829–1842, https://doi.org/10.1016/j.jcmgh.2022.02.011.
[40] A. Andrew, Intestinal endocrine cells of chicks around the time of hatching, Cell Tissue Res 172 (1976) 541–551, https://doi.org/10.1007/BF00220338.
[41] W.J. Krause, J. Yamada, J.H. Cutts, Enteroendocrine cells in the developing opossum small intestine and colon, J. Anat. 162 (1989) 83–96.
[42] X.F. Hu, Y.M. Guo, B.Y. Huang, S. Bun, L.B. Zhang, J.H. Li, et al., The effect of glucagon-like peptide 2 injection on performance, small intestinal morphology, and nutrient transporter expression of stressed broiler chickens, Poult. Sci. 89 (2010) 1967–1974, https://doi.org/10.3382/ps.2009-00547.
[43] C. Mo, Y. Zhong, Y. Wang, Z. Yan, J. Li, Characterization of glucagon-like peptide 2 receptor (GLP2R) gene in chickens: functional analysis, tissue distribution, and developmental expression profile of GLP2R in embryonic intestine, Domest. Anim. Endocrinol. 48 (2014) 1–6, https://doi.org/10.1016/j.domaniend.2014.01.002.
[44] N. Reicher, T. Melkman-Zehavi, J. Dayan, Z. Uni, Intra-amniotic administration of l-glutamine promotes intestinal maturation and enteroendocrine stimulation in chick embryos, Sci. Rep. 12 (2022) 2645, https://doi.org/10.1038/s41598-022-06440-z.

[45] S. Arthur, P. Manoharan, S. Sundaram, M.M. Rahman, B. Palaniappan, U. Sundaram, Unique regulation of enterocyte brush border membrane Na-glutamine and Na-alanine co-transport by peroxynitrite during chronic intestinal inflammation, Int. J. Mol. Sci. 20 (2019) 1504, https://doi.org/10.3390/ijms20061504.

[46] W. He, K. Furukawa, C.A. Bailey, G. Wu, Oxidation of amino acids, glucose, and fatty acids as metabolic fuels in enterocytes of post-hatching developing chickens, J. Anim. Sci. 100 (2022) skac053, https://doi.org/10.1093/jas/skac053.

[47] D. Li, X. Dang, H. Xu, H. Zhou, Y. Lou, X. Liu, et al., Growth performance, jejunal morphology, disaccharidase activities, and sugar transporter gene expression in Langde geese as affected by the in ovo injection of maltose plus sucrose, Front. Vet. Sci. 10 (2023) 1061998, https://doi.org/10.3389/fvets.2023.1061998.

[48] X. Dang, H. Zhou, Y. Lou, D. Li, Effects of methionine and/or disaccharide injected in the amnion of geese on post-hatching pectoral muscle and small intestine development, glycogen reserves, jejunum morphology, and digestive enzymes activities, Poult. Sci. 101 (2022) 101867, https://doi.org/10.1016/j.psj.2022.101867.

[49] J. Arevan, A. Sadeghi, A. Karimi, Effect of iof and its interaction with post-hatch feeding procedure on hatchability, some organs development and post-hatch performance in broiler chickens, Vet. Med. Sci. 9 (2023) 1269–1280, https://doi.org/10.1002/vms3.1121.

[50] J. Huang, L. Zhang, C. He, Y. Qu, J. Li, J. Zhang, et al., Claudin-1 enhances tumor proliferation and metastasis by regulating cell anoikis in gastric cancer, Oncotarget 6 (2015) 1652–1665, https://doi.org/10.18632/oncotarget.2936.

[51] S.T. Ballard, J.H. Hunter, A.E. Taylor, Regulation of tight-junction permeability during nutrient absorption across the intestinal epithelium, Annu. Rev. Nutr. 15 (1995) 35–55, https://doi.org/10.1146/annurev.nu.15.070195.000343.

[52] T. Vanuytsel, J. Tack, R. Farre, The role of intestinal permeability in gastrointestinal disorders and current methods of evaluation, Front. Nutr. 8 (2021) 717925, https://doi.org/10.3389/fnut.2021.717925.